Journal of Materials Chemistry C

This article can be cited before page numbers have been issued, to do this please use: S. D. Worrall, M. A. Bissett, W. Hirunpinyopas, M. Attfield and R. Dryfe, *J. Mater. Chem. C*, 2016, DOI: 10.1039/C6TC03496A.

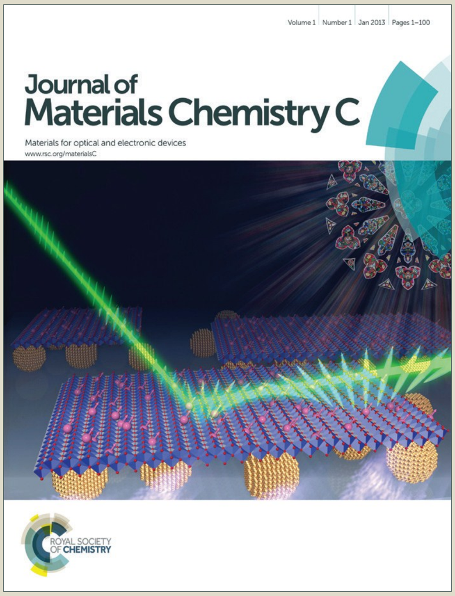

Journal of Materials Chemistry C

View Article Online
DOI: 10.1039/C6TC03496A

PAPER

Facile fabrication of metal-organic framework HKUST-1-based rewritable data storage devices

Stephen D. Worrall,[a,b] Mark A. Bissett,[c] Wisit Hirunpinyopas,[b] Martin P. Attfield*[a,b] and Robert A. W. Dryfe*[b]

Received 00th January 20xx,
Accepted 00th January 20xx

DOI: 10.1039/x0xx00000x

www.rsc.org/MaterialsC

Metal-organic framework (MOF) HKUST-1 coated Cu electrodes synthesised by a quick and scalable anodic dissolution process and assembled into a sealed, symmetrical, two electrode coin cell configuration are shown to demonstrate redox-based data storage behaviour. The observed behaviour is confirmed to be definitively due to the HKUST-1 itself as opposed to the underlying Cu/CuO electrode surface by demonstration of the same effect using HKUST-1/PVDF composite coated carbon fibre electrodes. This data storage behaviour is attributed to the immobilisation of a fixed number of electrically accessible active Cu cations within the porous HKUST-1 framework that are in the vicinity of the electrode surfaces and their ability to undergo facile $Cu^{2+/+}$ redox interconversion as a function of the potential applied across the electrodes. This proposed redox-based mechanism for the observed data storage effect has never previously been reported for MOF-based devices. Optimisation of electrolyte composition, electrolyte concentration and electrode separation results in "on"/"off" curent densitites of the order of 1 mA cm^{-2} , an "on":"off" ratio of ~ 5, "on"/"off" states stable to at least 10 consecutive reads, rewritability that persists over 6000 cycles, and the storage of data that can still be read hours after writing. The resulting data storage devices are more stable to successive reading and can be rewritten many more times than other previously reported pure MOF-based devices.

1. Introduction

Porous metal-organic frameworks (MOFs) are a class of nanoporous, crystalline material composed of metal ions, or metal - containing inorganic clusters, linked together by heteroatom containing organic molecules to form 3-dimensional structures.[1] These structures exhibit pores that propagate through the structure in one, two or three dimensions, imparting these materials with exceptionally high porosities and specific surface areas.[1] Since the synthesis of the first MOF, that could maintain porosity in the absence of guest molecules in the pore network,[2] huge research interest has focussed on investigating the many and varied potential applications of these novel materials.[3-11]

An application of MOFs that has received comparatively little attention is in data storage. The limited research that has been done has demonstrated the possibility of utilising pure MOFs,[12, 13] MOF composites,[14] MOF derived materials[15] and similar metal organic compounds[16, 17] to fabricate devices for electrically addressable data storage that rely on being able to change resistance between a low "on" and high "off" state. Such devices are often referred to as resistive memory devices or "memristors".[18] Switching between the two states, and determining which state the device is in, are both achieved by application of a potential. Usually a significantly higher "writing" potential is required to switch states than to determine a state.[18] When determining a state a "reading" potential is applied and the current is recorded, a high current corresponding to a low resistance "on" state and a low current corresponding to a high resistance "off" state. The mechanisms by which these devices switch between their high and low resistance states upon application of a high "writing" potential vary.[18]

In some devices the applied potential chemically converts an active material on or between the electrodes into a different phase, or different material, with a different resistance.[12, 14-16, 19, 20] If the conversion is reversible then the device is rewritable, however if it is irreversible then once the device has been written into a state it cannot be changed. Such devices are referred to as Write Once Read Many (WORM) devices.[14] In other devices, referred to as Redox-Based Resistive Switching Memories (ReRAMs), the high resistance "off" state and low resistance "on" state are interconverted by the reversible formation and destruction of

---

[a] *Centre for Nanoporous Materials, School of Chemistry, University of Manchester, Oxford Road, Manchester, M13 9PL, U. K.*
[b] *School of Chemistry, University of Manchester, Oxford Road, Manchester, M13 9PL, U. K.*
[c] *School of Materials, University of Manchester, Oxford Road, Manchester, M13 9PL, U. K.*
E-mail: m.attfield@manchester.ac.uk; robert.dryfe@manchester.ac.uk

Electronic Supplementary Information (ESI) available: A schematic of the electrochemical synthesis process, PXRD, Raman and SEM characterisation, calculation of charge transferred, electrolyte conductivity measurements and additional stability and rewritability measurements. See DOI: 10.1039/x0xx00000x

View Article Online
DOI: 10.1039/C6TC03496A

an electrically conductive filament grown between the two electrodes as a function of the applied potential.[17, 21, 22] When the filament is only in contact with one electrode then the device has a high resistance, but as soon as the filament contacts the second electrode the device essentially shorts leading to a much lower resistance. A recent publication has demonstrated that a similar effect is possible without the formation of a filament connecting both electrodes, but instead through the formation of a network of un-connected metal nanoparticles dispersed in a porous material.[13] These Ag nanoparticles provide a pathway for electrons to pass through the porous ZIF-8 from one electrode to the other via a hopping type mechanism.[13] The system is also shown to be environmentally responsive, with the high resistance state shown to vary significantly dependent upon the atmospheric contact of a variety of organic molecules.[13] MOFs as thin films possess intrinsic advantages over MOFs in other forms when it comes to attempting to integrate them into electronic devices. Other recent work has demonstrated the use of the pure MOF HKUST-1, in the form of a SURMOF (surface-anchored MOF) thin film sandwiched between two electrodes, as a resistive solid state memory device.[23] Interestingly the device operates within a much lower potential window (±1 V) than previously reported MOF based resistive memory devices.[23] At this stage the mechanism that causes this reversible change in resistance at low bias potential is not fully understood. The effect becomes more pronounced when ferrocene is incorporated into the pores of the HKUST-1 but, as the effect is also observed when pure HKUST-1 is used, it appears that it is possible for the MOF itself to be entirely responsible for the observed effect.[23]

An alternative method for obtaining a well adhered film of HKUST-1 in direct contact with an electrode material is the anodic dissolution method.[24] Application of a potential sufficient to oxidise Cu to Cu^{2+}, between two Cu electrodes immersed in an electrolyte solution containing 1,3,5-benzenetricarboxylic acid (BTC) leads to the formation of a coating of HKUST-1 on the anode surface. Fig. 1 shows the paddle wheel structure that the Cu^{2+} ions and BTC anions adopt within the HKUST-1 framework. Previous work has shown that when immobilised onto an electrode surface it is possible to use cyclic voltammetry to perform the redox interconversion, $Cu^{2+/+}$ on the Cu^{2+} in the immobilised framework.[25] Other reports have also seen similar behaviour in BTC MOFs containing other metals such as $Fe^{3+/2+}$.[26] For these redox interconversions to be performed as function of the applied potential the metal cations in the MOF crystals must be electrically accessible. Due to the low conductivity of these MOFs it is logical to assume that only the metal cations closest to the underlying electrode surface, the MOF/electrode interface (MEI), undergo the redox reaction.

Here we demonstrate that HKUST-1 coated Cu electrodes synthesised by facile, quick, scalable anodic dissolution and assembled into a sealed, symmetrical, two electrode coin cell configuration exhibit redox based, rewritable data storage behaviour. The resulting data storage devices are more stable to successive reading and can be rewritten many more times than other previously reported pure MOF-based devices. We also show the active material in the device is the HKUST-1 and attribute the data storage behaviour to the immobilisation of a fixed number of electrically accessible Cu cations within the porous HKUST-1 framework itself that are in the vicinity of the electrode surfaces.

.

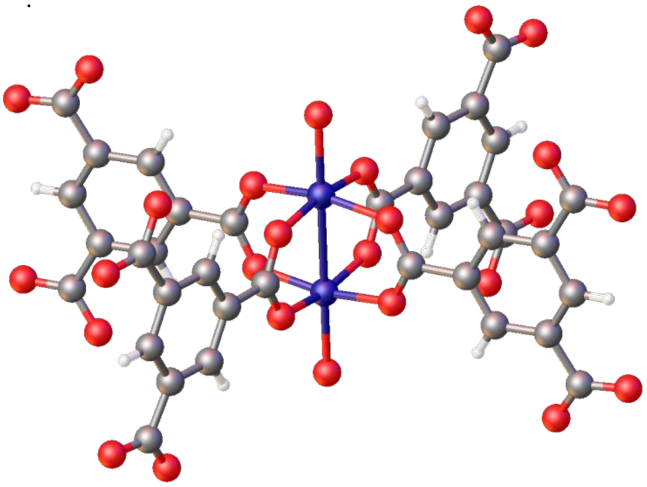

Fig. 1 Paddle wheel structure adopted by Cu^{2+} cations and BTC anions within the HKUST-1 framework. Copper is represented in blue, oxygen in red, carbon in grey and hydrogen in white.[27]

2. Experimental

2.1. Materials

Cu (Oxygen Free High Conductivity) foil, 1-methyl-2-pyrrolidone (NMP) (≥99%) and tetraethylammonium tetrafluoroborate (TEATFB) (99%) were obtained from Alfa Aesar. Acetonitrile (HPLC grade) was obtained from Fisher Scientific. Ultra-pure water (18.2 MΩ cm resistivity) was obtained from a Milli-Q Millipore Direct 8 purification unit. 1,3,5–benzenetricarboxylic acid (BTC) (95%), ethanol (≥99.8%) methanol (≥99.8%), poly(vinylidene fluoride), sodium sulphate (≥99%), tributylmethylammonium methyl sulphate (TBMAMS) (≥95%) and Whatman Grade 1 Qualitative Filter Paper were obtained from Sigma Aldrich. All materials were used as received.

2.2. HKUST-1 coating synthesis

HKUST-1 coatings were synthesised by immersing two Cu foil electrodes (geometric area ca. 16 cm^2), held approximately 2 cm apart into a heated solution of 48 mM BTC and 64 mM TBMAMS in 1:1 ethanol:H_2O. N_2 (g) was bubbled through in order to deaerate the solution. A PGSTAT302N Potentiostat (Metrohm Autolab B. V., The Netherlands) was used to apply a fixed potential difference of 2.5 V between the two Cu foil electrodes for 30 min, generating a coating of HKUST-1 on the anode surface (Shown schematically in the supporting information, Fig. S1). The coated anodes were rinsed three times with methanol post synthesis to remove unreacted linker and supporting electrolyte. HKUST-1 was also formed in solution during the synthesis; this material was filtered, washed three times with methanol and retained.

View Article Online
DOI: 10.1039/C6TC03496A

2.3. HKUST-1/PVDF composite electrode preparation

HKUST-1 powder (produced as a by-product during the HKUST-1 coating synthesis) was mixed in a 1:1 mass ratio with a 10 wt% PVDF in NMP solution. Further NMP was applied to dilute the composite sufficiently before it was drop cast onto a carbon fibre electrode (Le Carbone, UK, geometric area ca. 0.5 cm^2). The electrode was then heated at 70 °C until dry.

2.4. Characterisation of HKUST-1 coatings

The material coating the electrode, and the material produced in solution, was confirmed as HKUST-1 using a PANalytical X'Pert X-ray diffractometer. Powder X-ray diffraction (PXRD) patterns were obtained from ground samples using Cu-Kα radiation at 40 kV and 30 mA, in the range 3-60 2θ° (with a step size of 0.017 2θ° and scan step time of 66 s) whilst spinning. Confocal Raman spectroscopy was also performed using a Renishaw inVia microscope with a 532 nm (2.33 ev) excitation at a power of 1 mW with a 100 objective, and a grating of 1800 l mm^{-1} to achieve a spectral resolution of 1 cm^{-1}.

The morphology and quality of the HKUST-1 coatings were characterised on the anode surface using a FEI Quanta 200 (Environmental) Scanning Electron Microscope ((E)SEM). All images were obtained at 20 kV, under low vacuum with a water vapour pressure of 0.83 Torr and utilising both secondary and backscattered Electron Detectors.

2.5. Preparation of HKUST-1 data storage devices

For initial open cell testing of the data storage effect, two ca. 16 cm^2 HKUST-1 coated Cu electrodes (ca. 10 cm^2 HKUST-1 coverage), or two ca. 16 cm^2 bare Cu electrodes were separated by Whatman Grade 1 Qualitative Filter Paper in either saturated Na_2SO_4 in 1:1 ethanol:H_2O or 1M TEATFB in acetonitrile. Three electrode analysis of the data storage effect was performed replacing one of the HKUST-1 coated Cu electrodes with a C rod counter electrode and a Ag wire "pseudo" reference electrode.

For subsequent, and longer term, closed cell analysis two ca. 1 cm^2 HKUST-1 coated Cu electrodes (ca. 1 cm^2 HKUST-1 coverage) were stacked front-to-front inside a sealed symmetrical coin cell (CR2032), separated by Whatman Grade 1 Qualitative Filter Paper and soaked in either saturated Na_2SO_4 in 1:1 ethanol:H_2O or 1M TEATFB in acetonitrile. In some devices the electrodes were replaced with ca. 0.5 cm^2 HKUST-1/PVDF composite coated carbon fibre electrodes.

The conductivity of the aqueous and non-aqueous electrolyte solutions was measured using a Mettler Toledo Seven Compact Conductivity Meter every 10 s for 10 minutes to obtain a stable reading. The conductivity of the solvents without the presence of the electrolyte was also obtained every 10 s for 5 minutes.

2.6. Operation of HKUST-1 data storage devices

HKUST-1 data storage devices were operated using both cyclic voltammetry and chronoamperometry. Cyclic voltammetry, used to both activate devices and switch them between "on" (high current) and "off" (low current) states, was performed in the range -0.8 to 0.8 V, the step potential was -0.61 mV and the scan rate varied from 0.07 to 2 V s^{-1}. Chronoamperometry, used to detect whether devices were in "on" (high current) or "off" (low current) states, was performed by applying a potential of between 0.2 and 0.5 V (device dependent) and recording the current once every 0.01 s for 0.1 s.

3. Results and Discussion

3.1. Characterisation of HKUST-1 coated electrodes

PXRD (Fig. S2a) confirms that the coating obtained on the electrode is highly crystalline HKUST-1 as reported previously.[24] The Raman spectra (Fig. S2b) obtained also match that observed previously for HKUST-1.[28] SEM images taken using a secondary electron detector (Fig. S2c) corroborate that the coating is made up of good quality crystals that display the octahedral morphology typical of cubic HKUST-1.[24] SEM images taken using the backscattered detector (Fig. S2d) highlight that the crystals in the coating are well intergrown as the apparent absence of brighter areas in the image indicates that there is little to no exposed metal surface.

3.2. Open cell testing

Comparing the cyclic voltammograms obtained in saturated Na_2SO_4 in 1:1 ethanol:H_2O, when using HKUST-1 coated Cu electrodes as opposed to bare Cu electrodes, in the open cell set up (as described in Section 2.5) indicates that the redox response seen is due to the HKUST-1 coating (Fig. 2). Whilst there is some, small Faradaic response that can be observed in the case of the bare Cu electrodes the magnitude of the peaks observed for the HKUST-1 coated Cu electrodes is significantly greater. This is to be expected if the observed behaviour is indeed due to the $Cu^{2+/+}$ pair, as whilst there will be a small concentration of Cu^{2+}/Cu^{+} species present in the form of oxides on the bare Cu surface, the concentration of Cu^{2+} present at the electrode surface, once the electrode is coated in a ~ 10µm thick coating of HKUST-1 will be much greater.

It has been demonstrated previously in a three electrode set up, that a HKUST-1 coated electrode displays a well-defined pair of peaks at a formal potential of ca. -0.1 V vs. Ag/AgCl, assigned to the $Cu^{2+/+}$ couple.[25] As the cyclic voltammograms recorded here were acquired using a two electrode set up it is not possible to accurately define the exact potential at which the observed peaks occur; however we can approximate that, as the cell is symmetrical, both electrodes experience half of the magnitude of the applied potential.[29] As the applied potentials at which the peaks occur are ca. -0.25 and 0.25 V we can estimate that the potential differences across each electrode/electrolyte interface are *ca.* -0.125 and 0.125 V, respectively. As these values are not referenced to Ag/AgCl we cannot compare them directly with the formal potential obtained from a three electrode system, but the fact that the $Cu^{II/I}$ couple was the only one observed in the three electrode cyclic voltammetry strongly suggests that the peaks observed in Fig. 2 are due to the same redox couple. A schematic explanation for the observed cyclic voltammetry is given in Fig. 3.

View Article Online
DOI: 10.1039/C6TC03496A

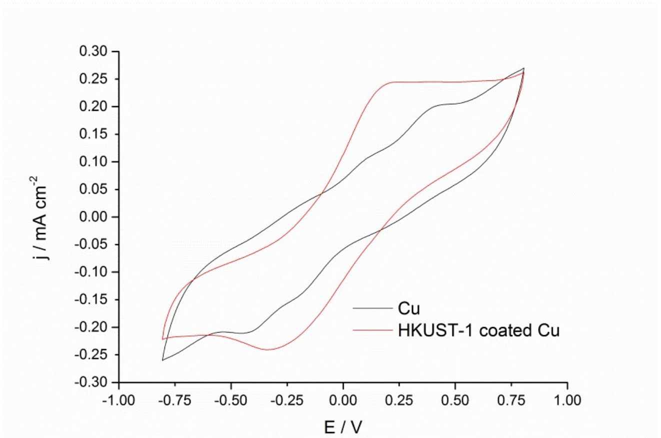

Fig. 2 Comparison of the cyclic voltammograms obtained when using HKUST-1 coated Cu electrodes as both the anode and cathode, separated by Whatman Grade 1 Qualitative Filter Paper in a two electrode system as opposed to bare Cu electrodes. Saturated Na_2SO_4 in 1:1 ethanol:H_2O; 0.07 V s^{-1}. Current density defined relative to the geometric area of the underlying Cu electrode.

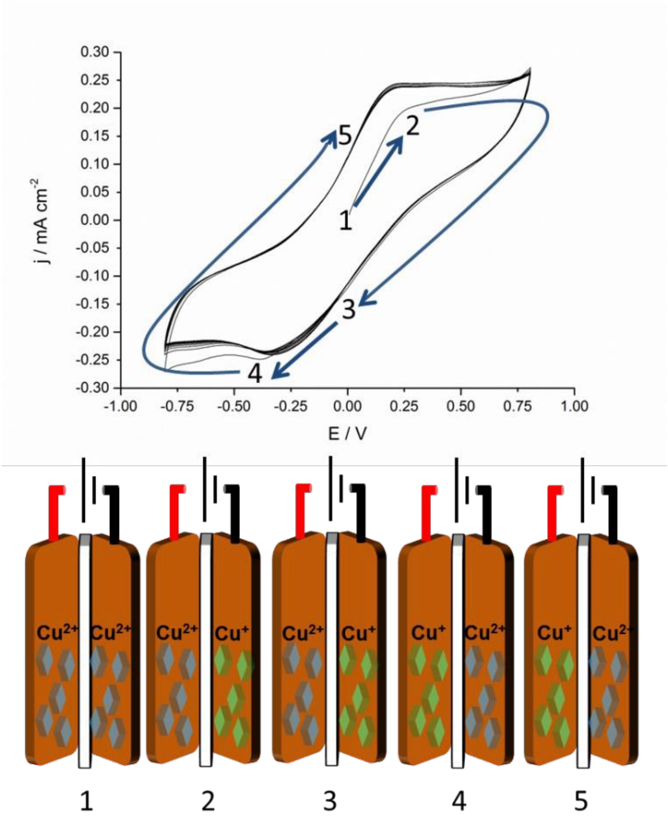

Fig. 3 Ten successive cyclic voltammograms obtained when using HKUST-1 coated Cu electrodes as both the anode and cathode, separated by Whatman Grade 1 Qualitative Filter Paper, in a two electrode system. Saturated Na_2SO_4 in 1:1 ethanol:H_2O; 0.07 V s^{-1} (top). Proposed mechanism behind the observed cyclic voltammetry of HKUST-1 coated Cu electrodes in a symmetrical, two electrode configuration. Cu^{2+} in HKUST-1 at the MEI is represented in blue and Cu^{+} in HKUST-1 at the MEI in green (bottom). Current density defined relative to the geometric area of the underlying Cu electrode.

At zero applied potential (1) the Cu ions in the HKUST-1 coatings at the MEI on both electrodes are in the 2+ oxidation state. As the potential is cycled slowly positive (2) the Cu^{2+} in the HKUST-1 coating at the MEI on the right hand electrode (RHE) is reduced to Cu^{+} whilst an oxidation occurs on the left hand electrode (LHE), probably related to the formation of surface oxide species on the underlying Cu (see Fig. 2). Then, as the potential is cycled back to zero (3), the system is unchanged. When the potential is then reversed and cycled slowly negative (4) the Cu^{+} in the HKUST-1 coating at the MEI on the RHE is oxidised back to Cu^{2+} and the Cu^{2+} in the HKUST-1 coating at the MEI on the LHE is reduced to Cu^{+}. Once again as the potential is cycled back to zero (5) the system is unchanged. The system can then be cycled repeatedly through steps 2 to 5, switching the system repeatedly from having Cu^{+} on the RHE and Cu^{2+} on the LHE, to having Cu^{2+} on the RHE and Cu^{+} on the LHE. The reason for the lower peak current on the first cycle of the device to step (2), compared to subsequent cycles (Fig. 3, top) is that the current flow is limited by the fact that the Cu cations in the HKUST-1 at the MEI on the LHE are unable to undergo oxidation in this cycle as they are already in the 2+ state.

The fact that the system remains unchanged as it is cycled back to 0 V (steps 3 and 5) leads to the possibility of rewritable data storage. If, rather than cycling through steps 2 – 5 in sequence the system is cycled through steps 4 and 5 twice in a row, we observe the cyclic voltammetry shown in Fig. 4.

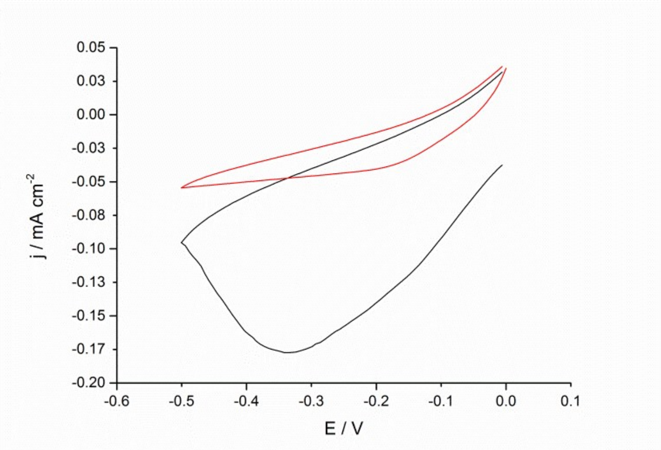

Fig. 4 Successive cyclic voltammograms obtained when using HKUST-1 coated Cu electrodes as both the anode and cathode, separated by Whatman Grade 1 Qualitative Filter Paper, in a two electrode system. First cycle in black and second cycle in red. Saturated Na_2SO_4 in 1:1 ethanol:H_2O; 0.07 V s^{-1}. Current density defined relative to the geometric area of the underlying Cu electrode.

The peak observed previously is present in the first cycle, but in the second cycle this feature is no longer visible. This is consistent with the proposed mechanism. In the first cycle (black) the Cu^{2+} in the HKUST-1 at the MEI on the LHE is reduced to Cu^{+} whilst on the RHE the Cu^{+} in the HKUST-1 at the MEI is oxidised to Cu^{2+}. Together these processes give rise to the observed peak. However in the second cycle (red) there is already Cu^{+} on the LHE and Cu^{2+} on the RHE which explains why no peak is observed. Using three electrode cyclic voltammetry (Fig S3a) the amount of charge passed is

View Article Online
DOI: 10.1039/C6TC03496A

calculated from the peak area. This was then used to calculate the number of Cu ion redox reactions this would correspond to and then, finally, the number moles of Cu^{2+} ions that are electrically accessible (see Supporting Information). According to these calculations ca. 0.4 µmol of Cu^{2+} ions are electrically accessible, which is significantly lower than the ca. 539 µmol present in the ca. 100 mg of HKUST-1 coating. This indicates that only ca. 0.7% of the Cu^{2+} ions in the HKUST-1 coating are involved in the redox process. This supports the assertion that, as HKUST-1 is a poor conductor with a large band gap,[30] only those Cu^{2+} ions closest to the underlying electrode surface, the MEI, undergo the redox reaction.

The fact that different peak current values are observed dependent on which way the system was cycled previously (Fig 4), allows for the storage of rewritable data. Defining cycling negative (steps 4 and 5) as writing “on”, cycling positive (steps 2 and 3) as writing “off” and applying a small positive voltage and recording the current as reading a state, provides a protocol for assessing the stability or rewritability of this HKUST-1 redox-based rewritable data storage device (see Fig. 5). Utilising this protocol the stability of written “on” and “off” states, to being repeatedly read was assessed in two different electrolyte solutions and the results can be seen in Fig. 6.

In both the aqueous and non-aqueous electrolyte solutions, very similar behaviour is observed with repeated reading of an “on” state (Fig 6a and c). The initial high peak current value recorded on the first read reduces rapidly with successive reads until, at around the 10th reading, it becomes indistinguishable from the low peak current value of the “off” state. It is supposed that an “on” state in both electrolytes has an initial high peak current because the Cu^+ in the HKUST-1 at the MEI on the LHE is being oxidised to Cu^{2+}, and the Cu^{2+} in the HKUST-1 at the MEI on the RHE is being reduced to Cu^+ as a result of the potential applied to read the state. With successive reads this process progresses towards completion such that at approximately the 10th reading all of the electrically accessible Cu cations have either been reduced or oxidised depending upon which electrode they are on, and the current observed is just that of the background.

In contrast, with successive reading of the “off” state (Fig 6a and c) different behaviour is observed dependent upon the electrolyte solution. In the lower conductivity (~ 3 mS cm^{-1}) saturated Na_2SO_4 in 1:1 ethanol:H_2O (Fig. 6a) the “off” state shows very little variation with successive reads; in contrast in the higher conductivity (~ 54 mS cm^{-1}) 1M TEATFB in acetonitrile the “off” state displays the inverse behaviour to the “on” state (see Fig. S4 for conductivity measurements). Starting at a low peak current value it then increases rapidly with successive reads before becoming indistinguishable from the “on” state after around 10 reads. This behaviour is consistent with the proposed mechanism. When the system is in the “off” state, in the lower conductivity saturated Na_2SO_4 in 1:1 ethanol:H_2O (Fig 6a), the current observed with successive reads changes little. This is because, as the Cu cations in the HKUST-1 at the MEI on the LHE and RHE are already in the Cu^{2+} and Cu^+ states respectively, nothing happens when the read potential is applied. As a result only the background current is observed at every read. It should be noted that this background current is reasonably high due to capacitive charge storage at the electrode/electrolyte interface. The reason that in the higher conductivity 1M TEATFB in acetonitrile in the “off” state shows the inverse behaviour to the “on” state is due to a “self-discharge” type process (Fig 6c). Inspection of the CV in Fig. 2 reveals that the observed current is already rising in both directions at 0 V. This implies that the $Cu^{2+/+}$ redox reaction is able to occur at zero bias, which means that when no potential is being applied the Cu^{2+} in the HKUST-1 at the MEI on the LHE can be reduced to Cu^+ and the Cu^+ in the HKUST-1 at the MEI on the RHE can be oxidised to Cu^{2+}. This results in the observed increase in the “off” current with successive reads. Whilst it is not possible to prevent the $Cu^{2+/+}$ redox reaction occurring at zero bias, by using the lower conductivity electrolyte solution the resistance of the device is increased. This significantly slows the rate of the $Cu^{2+/+}$ redox reaction at zero bias, giving rise to the observed stable behaviour of the “off” state in the lower conductivity electrolyte (Fig 6a).

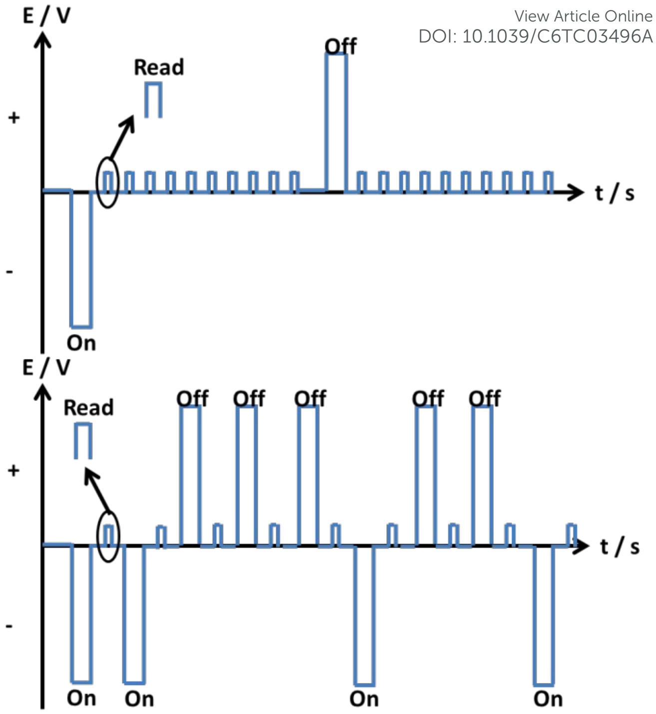

Fig. 5 Illustration of the potential steps performed for stability testing (top) and rewritability testing (bottom). For stability testing (top) an “on”, or “off”, state is “written” by cycling from 0 V to a high negative, or positive, potential and back to 0 V. A small positive “read” potential is then applied in order to read the device, a high current means the device is in a “on” state and a low current means it is in an “off” state. This “read” potential is then applied 9 more times, with a 1 minute gap between each “read”. For rewritability testing (bottom) the same processes are applied but rather than “writing” the device once and “reading” it many times as in the stability test (top) the device is “rewritten” after every “read”. Only the first 9 cycles of rewritability are shown

View Article Online
DOI: 10.1039/C6TC03406A

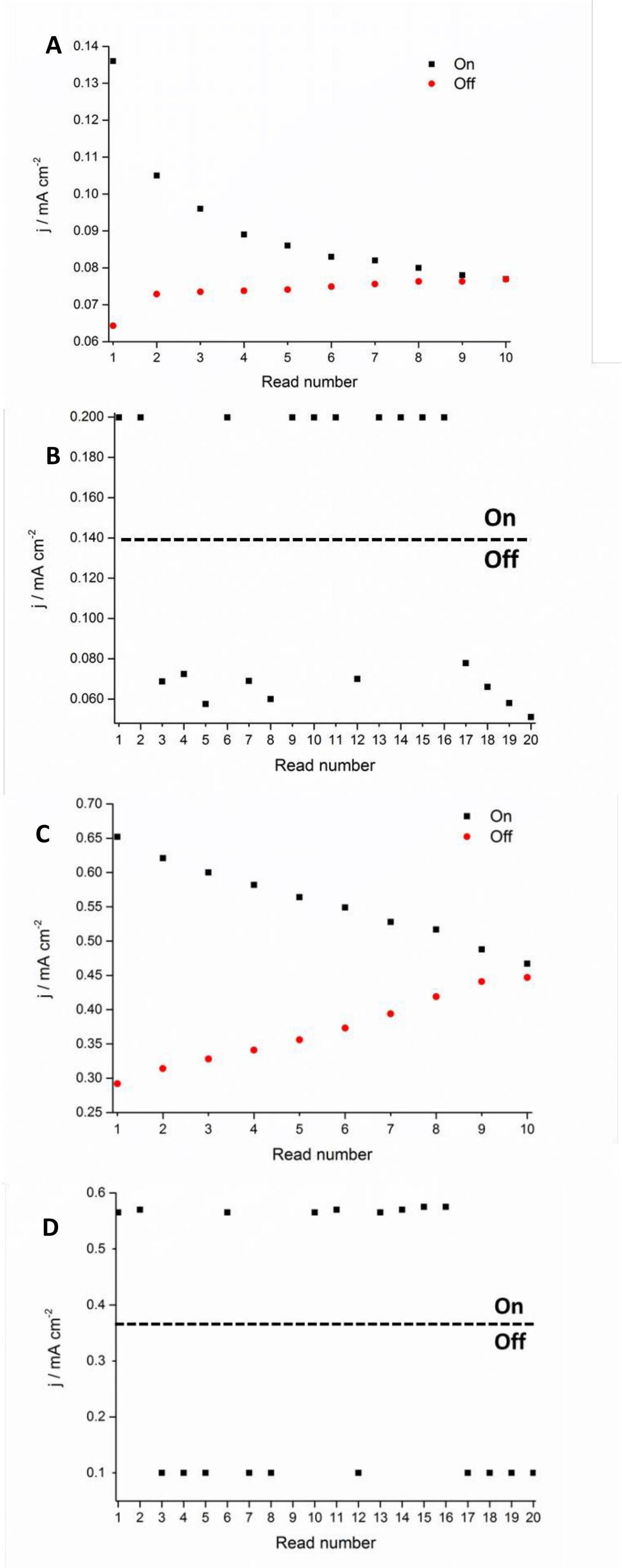

Fig. 6 Stability (A and C) and rewritability (B and D) of “on” and “off” states written (at 0.07 V s^{-1}) and read according to the potential step process outlined in Fig. 5. Current densities (j) obtained from chronoamperometry in saturated Na_sSO_4 in 1:1 ethanol:H_2O (A and B) or 1M TEATFB in acetonitrile (C and D).

The effect of writing the “on” and “off” states at scan rates faster than 0.07 V s^{-1} was also assessed (Fig. S5). At the slowest scan rate (0.07 V s^{-1}) the “on”:”off” ratio is ~ 2.11 (Fig 6a), whilst at the fastest scan rate (2 V s^{-1}) it is ~ 1.67 (Fig S5). This again is consistent with the proposed mechanism, as if a slower scan rate is used to write a state the Cu$^{2+/+}$ redox processes on the LHE and RHE will have progressed further than if a faster scan rate was used. This effect is also apparent when assessing the rewritability of the system at the same range of scan rates. As the slower scan rate was demonstrated to give the best results all subsequent experiments were done with “on” and “off” states written at 0.07 V s^{-1}.

Whilst we have established that a lower conductivity electrolyte helps stabilise the written “off” states it does also have a negative impact upon the observed “on”:”off” ratio (Fig 6b and d), In the lower conductivity electrolyte (Fig 6b) the maximum “on”:”off” ratio is ~ 3 whilst in the higher conductivity electrolyte it is > 5. This again is consistent with the proposed mechanism, as if a higher conductivity electrolyte is used the Cu$^{2+/+}$ redox processes on the LHE and RHE will have progressed further in a given time than if a lower conductivity electrolyte was used. The rewritability of the system is not significantly affected by the electrolyte solution as in both cases it is possible to write an “on” or “off” state, read correctly whether it was an “on” or “off” state and then write another “on” or “off” state, at least twenty times. Longer term testing of the rewritability of the system was not possible using the open cell set up due to solvent evaporation, so further testing was performed using a closed coin cell set up.

3.3. Coin cell testing

A schematic of the sealed coin cell architecture is shown in Fig. 7. Initially the effect of the number of separators used in the coin cell set up upon the data storage system was investigated. Coin cells were prepared with 1, 2 and 4 separators and cyclic voltammetry was used to assess the behaviour of the different devices (Fig. S6). The fewer the number of separators, the smaller the inter electrode separation and the greater the observed current density. Potentially of more interest however is the observed increase in peak-to-peak separation with increasing number of separators. It is clear that the peaks are being significantly broadened as well as shifted and therefore this behaviour is attributed to the increasing resistance of the device with the increasing number of separators.

It was discovered, when assessing the stability and rewritability of coin cell devices prepared using both the previously used electrolyte solutions, that the best stability and rewritability using the coin cell system was obtained when the larger number of separators was used so the resistance of the system was higher (Fig. 8). This corroborates with the positive effect that the lower conductivity electrolyte had upon the stability of the “off” states in the open cell set up. The effect on the stability of the stored data was the most pronounced, with “on” and “off” states still clearly distinguishable after 10 successive reads when using a larger

View Article Online
DOI: 10.1039/C6TC03496A

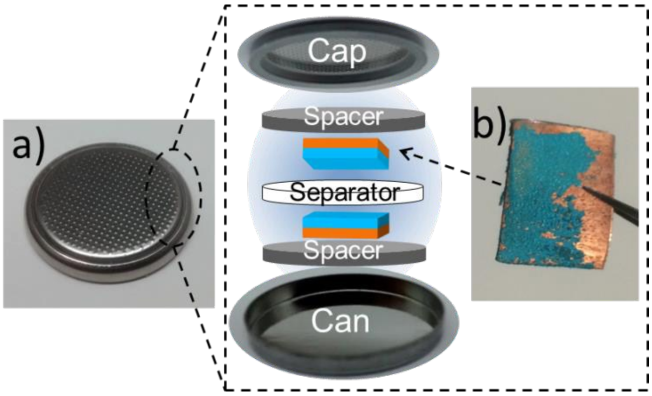

Fig. 7 Photograph of the external casing of a coin cell, with a blown up illustration of the arrangement of the components in a HKUST-1 data storage device, (A) and a photograph of a HKUST-1 coated Cu electrode (B).

number of separators. This is consistent with the proposed mechanism for the memory effect. A higher resistance across the device will reduce the rate at which the Cu$^{2+/+}$ redox process occurs when applying the potential to read a state, thus allowing for a greater number of successive reads before the reaction is complete and the “on” and “off” states become indistinguishable from each other.

The main reason for switching from the open cell to the coin cell system was in order to investigate the data storage effect exhibited by the HKUST-1 coated Cu electrodes over hours as opposed to just minutes. This did not prove possible using the 1M TEATFB in acetonitrile electrolyte as, regardless of whether an “on” or “off” state was written, after waiting ~ 1 hour it was not possible to distinguish between the states. This was attributed to the “self-discharge” process discussed previously. However, using the saturated Na$_2$SO$_4$ in 1:1 ethanol:H$_2$O successively enabled the storage of data to persist over hours as opposed to just minutes. Fig. 9 shows that an “on” or “off” state written 6 hours previously can still be identified correctly as an “on” or “off” state. This also demonstrates the reproducibility of the 6 hour stability. A device can go through at least 4 cycles of writing an “on” or “off” state, waiting 6 hours and then reading the state back successfully. This also demonstrates that a device is still operational 24 hours after the first use.

To verify that the observed effect was definitively due to the HKUST-1 coating, and not due to other factors such as increased quantities of copper oxides at the electrode surface as a result of the coating process, coin cell devices prepared using HKUST-1 drop cast onto carbon cloth electrodes (and bare carbon cloth electrodes) were also tested. Comparing the cyclic voltammetry of the HKUST-1 coated carbon cloth with that of the blank carbon cloth definitively demonstrates that the observed behaviour is due to the HKUST-1 coating; the stability and rewritability of the written “on” and “off” states is also very similar to that observed when using HKUST-1 coated Cu electrodes (Fig. S7).

As well as testing the long term stability of the data stored using the coin cell based device the rewritability of the device over the long term was also tested. Fig. 10 shows the cyclic

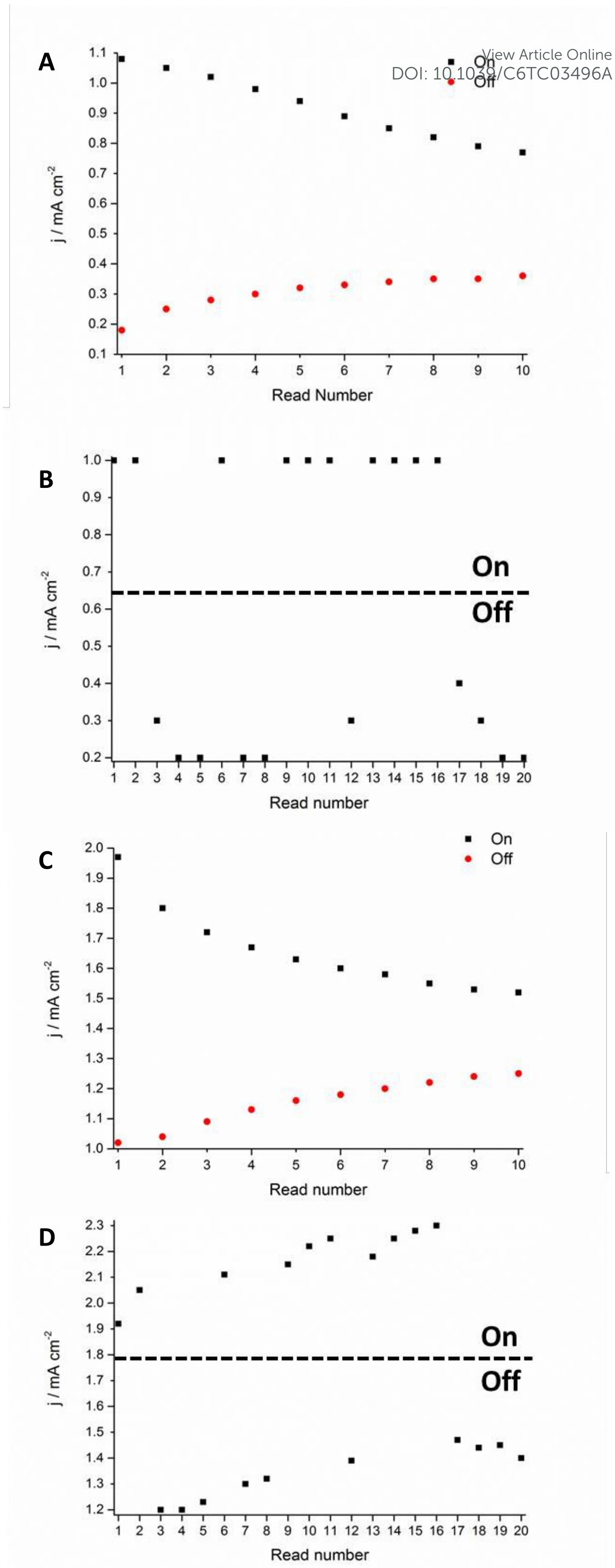

Fig. 8 Stability (A and C) and rewritability (B and D) of “on” and “off” states, written (at 0.07 V s^{-1}) and read according to the potential step process outlined in Fig. 5. Current densities (j) obtained from chronoamperometry in saturated Na$_s$SO$_4$ in 1:1 ethanol:H$_2$O (A and B) or 1M TEATFB in acetonitrile (C and D). 5 separators were used in the device.

View Article Online
DOI: 10.1039/C6TC02496A

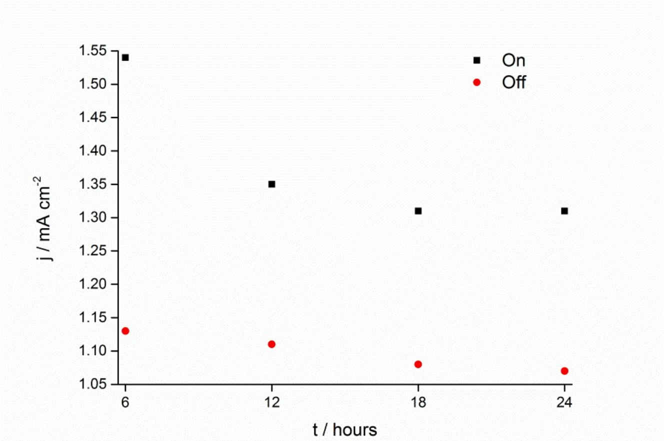

Fig. 9 Longer term stability of “on” and “off” states, written at 0.07 V s^{-1} in a coin cell. Current densities j obtained from chronoamperometry in saturated Na_2SO_4 in 1:1 ethanol:H_2O. The “on” or “off” state was rewritten after each read.

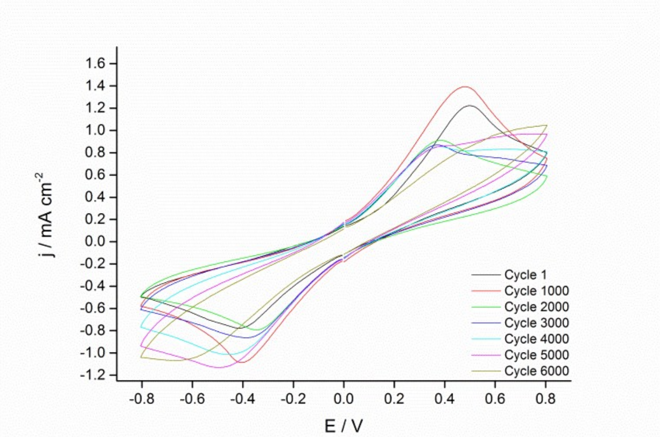

Fig. 10 Change in the observed cyclic voltammetry of a HKUST-1 coated Cu electrode coin cell device with increasing cycle number. Data obtained in saturated Na_2SO_4 in 1:1 ethanol:H_2O at 0.07 V s^{-1}.

voltammograms used to write the 1st ”on” and “off” state in a device and then every 1000th “on” and “off” state up to the 6000th “on” and “off” state. Comparing the 1st and 1000th cycles the observed redox peaks become sharper and more intense, however by the 2000th cycle the peaks have begun to broaden and reduce in intensity. This trend towards broader and less intense peaks then continues with increasing cycle number. Whilst the cyclic voltammetry of the coin cell device does change significantly, with the observed peaks becoming broader and less intense, the peaks are still present; thus the device is still operational after over 6000 cycles. This initial improvement in electrochemical behaviour, sharper peaks and higher currents, over the first 1000 cycles could be due to improved wetting of the HKUST-1 coated Cu electrode due to increased permeation of the electrolyte into the porous structure with successive cycling. Similar behaviour has been previously reported for other materials in general when exposed to such cycling and particularly in similar coin cell type devices.[31] PXRD analysis (Fig. S8a) shows that after all this cycling a significant proportion of the HKUST-1 coating has converted to another crystalline phase of Cu^{2+} and BTC[32] and that significant amounts of copper oxide species are now also present.[33] The presence of a mixed phase coating at the end of the cycling, which presumably built up progressively during cycling, potentially explains the peak broadening and reduction in current observed in the cyclic voltammetry from 1000 cycles onwards. SEM images of the electrode (Fig S8b and c) taken after the 6000 cycles corroborate the PXRD data, with large numbers of crystals of the morphology of the other crystalline phase of Cu^{2+} and BTC observed alongside HKUST-1 crystals and copper oxide deposits.

The results reported in this work are compared against the other pure MOF based data storage devices reported in the literature (Table 1). Whilst the “on”:”off” ratio reported here (~5) is lower than typically reported, a difference in current density of ~ 1 mA cm^{-2} is more than sufficient to reliably distinguish between “on” and “off” states. The redox based nature of the data storage mechanism in the device reported here necessarily limits the stability of the written “on” and “off” states to successive reading, but the number of readable cycles reported here of 10 compares favourably with values reported in the literature.[12, 23] The rewritability reported here of > 6000 cycles is the highest reported value for a pure MOF device. Finally, whilst the stability of the stored “on” and “off” states reported here of 6 hours is not as high as that reported in previous work, further optimisation of the system should improve this value. These easily prepared symmetrical, two electrode coin cell devices made from HKUST-1 coated Cu electrodes are able to compete with, and in some cases exceed, the properties of the more laboriously prepared single crystal and SURMOF based devices.

Table 1 Comparison of MOF-based data storage devices

	On:Off ratio	Stability to successive reading	Rewritability	Stability to time
Grzybowski[12]	> 150	10	> 20	> 1 week
Baumgart, Wöll and Edel [23]	~ 10	> 3	> 3	?
This work	~ 5	> 10	> 6000	~ 6 hours

Conclusions

HKUST-1 coatings on Cu electrodes, obtained using the quick and scalable anodic dissolution technique, and assembled into symmetrical electrochemical cells have been shown to exhibit redox based data storage behaviour. It has been demonstrated that the data storage effect is due to the HKUST-1 itself. The observed effect is due to the redox chemistry of the $Cu^{II/I}$ couple occurring on the Cu^{2+} ions immobilised within the HKUST-1 coating at the MEI. The presence of the MOF is crucial for the proposed mechanism as it provides a fixed concentration of immobilized Cu cations in the vicinity of the MEI that are necessary for a high read current in the “on” state. The devices within this system are significantly easier to fabricate and manipulate than other pure MOF based data storage devices and exhibit comparable or enhanced properties.

Acknowledgements

The authors would like to thank Dr Patrick Hill for his assistance with SEM. SDW would like to thank the NoWNANO DTC for funding and RAWD would like to thank the EPSRC (UK, grant references EP/K039547/1 and EP/K016954/1) for support. Additional research data supporting this publication are available as supplementary information accompanying this publication at [INSERT DOI].

References

1. G. Ferey, *Chem. Soc. Rev.*, 2008, **37**, 191-214.
2. H. Li, M. Eddaoudi, M. O'Keeffe and O. M. Yaghi, *Nature*, 1999, **402**, 276-279.
3. M. Meilikhov, K. Yusenko, D. Esken, S. Turner, G. Van Tendeloo and R. A. Fischer, *Eur. J. Inorg. Chem.*, 2010, 3701-3714.
4. S. B. Han, Y. H. Wei, C. Valente, I. Lagzi, J. J. Gassensmith, A. Coskun, J. F. Stoddart and B. A. Grzybowski, *J. Am. Chem. Soc.*, 2010, **132**, 16358-16361.
5. B. Levasseur, C. Petit and T. J. Bandosz, *ACS Applied Materials & Interfaces*, 2010, **2**, 3606-3613.
6. C. Lu, T. Ben, S. Xu and S. Qiu, *Angew. Chem. Int. Ed.*, 2014, **53**, 6454-6458.
7. R. Banerjee, A. Phan, B. Wang, C. Knobler, H. Furukawa, M. O'Keeffe and O. M. Yaghi, *Science*, 2008, **319**, 939-943.
8. A. R. Millward and O. M. Yaghi, *J. Am. Chem. Soc.*, 2005, **127**, 17998-17999.
9. A. Henschel, K. Gedrich, R. Kraehnert and S. Kaskel, *Chem. Commun.*, 2008, 4192-4194.
10. N. Campagnol, E. R. Souza, D. E. De Vos, K. Binnemans and J. Fransaer, *Chem. Commun.*, 2014, **50**, 12545-12547.
11. S. D. Worrall, H. Mann, A. Rogers, M. A. Bissett, M. P. Attfield and R. A. W. Dryfe, *Electrochim. Acta*, 2016, **197**, 228-240.
12. S. M. Yoon, S. C. Warren and B. A. Grzybowski, *Angew. Chem. Int. Ed.*, 2014, **53**, 4437-4441.
13. Y. Liu, H. Wang, W. Shi, W. Zhang, J. Yu, B. K. Chandran, C. Cui, B. Zhu, Z. Liu, B. Li, C. Xu, Z. Xu, S. Li, W. Huang, F. Huo and X. Chen, *Angew. Chem. Int. Ed.*, 2016, **128**, 9030-9034.
14. X. Huang, B. Zheng, Z. Liu, C. Tan, J. Liu, B. Chen, H. Li, J. Chen, X. Zhang, Z. Fan, W. Zhang, Z. Guo, F. Huo, Y. Yang, L.-H. Xie, W. Huang and H. Zhang, *ACS Nano*, 2014, **8**, 8695-8701.
15. L. Pan, Z. Ji, X. Yi, X. Zhu, X. Chen, J. Shang, G. Liu and R.-W. Li, *Adv. Funct. Mater.*, 2015, **25**, 2677–2685.
16. B.-B. Cui, Z. Mao, Y. Chen, Y.-W. Zhong, G. Yu, C. Zhan and J. Yao, *Chemical Science*, 2015, **6**, 1308-1315.
17. B. Radha, A. A. Sagade and G. U. Kulkarni, *Appl. Phys. Lett.*, 2014, **105**, 083103.
18. C. Tan, Z. Liu, W. Huang and H. Zhang, *Chem. Soc. Rev.*, 2015, **44**, 2615-2628.
19. Y.-F. Chang, B. Fowler, Y.-C. Chen, F. Zhou, C.-H. Pan, T.-C. Chang and J. C. Lee, *Scientific Reports*, 2016, **6**, 21268-21277.
20. K.-C. Chang, T.-C. Chang, T.-M. Tsai, R. Zhang, Y.-C. Hung, Y.-E. Syu, Y.-F. Chang, M.-C. Chen, T.-J. Chu, H.-L. Chen, C.-H. Pan, C.-C. Shih, J.-C. Zheng and S. M. Sze, *Nanoscale Research Letters*, 2015, **10**, 1-27.
21. I. Valov, *ChemElectroChem*, 2014, **1**, 26-36.
22. Y.-F. Chang, B. Fowler, Y.-C. Chen and J. C. Lee, *Prog. Solid State Chem.*, 2016, http://dx.doi.org/10.1016/j.progsolidstchem.2016.07.001
23. Z. Wang, D. Nminibapiel, P. Shrestha, J. Liu, W. Guo, P. G. Weidler, H. Baumgart, C. Wöll and E. Redel, *ChemNanoMat*, 2016, **2**, 67-73.
24. R. Ameloot, L. Stappers, J. Fransaer, L. Alaerts, B. F. Sels and D. E. De Vos, *Chem. Mater.*, 2009, **21**, 2580-2582.
25. J. J. Mao, L. F. Yang, P. Yu, X. W. Wei and L. Q. Mao, *Electrochem. Commun.*, 2012, **19**, 29-31.
26. K. F. Babu, M. A. Kulandainathan, I. Katsounaros, L. Rassaei, A. D. Burrows, P. R. Raithby and F. Marken, *Electrochem. Commun.*, 2010, **12**, 632-635.
27. S. S. Y. Chui, S. M. F. Lo, J. P. H. Charmant, A. G. Orpen and I. D. Williams, *Science*, 1999, **283**, 1148-1150.
28. C. Prestipino, L. Regli, J. G. Vitillo, F. Bonino, A. Damin, C. Lamberti, A. Zecchina, P. L. Solari, K. O. Kongshaug and S. Bordiga, *Chem. Mater.*, 2006, **18**, 1337-1346.
29. D. Plana, F. G. E. Jones and R. A. W. Dryfe, *J. Electroanal. Chem.*, 2010, **646**, 107-113.
30. C. H. Hendon and A. Walsh, *Chemical Science*, 2015, **6**, 3674-3683.
31. M. A. Bissett, I. A. Kinloch and R. A. W. Dryfe, *ACS Applied Materials & Interfaces*, 2015, **7**, 17388-17398.
32. R. Pech and J. Pickardt, *Acta Cryst. C*, 1988, **44**, 992-994.
33. S. L. Cheng and M. F. Chen, *Nanoscale Research Letters*, 2012, **7**, 119.